# A Versatile PC-Based Platform For Inertial Navigation

*Isaac Skog, Adrian Schumacher and Peter Händel*

Signal Processing Lab
Electrical Engineering
Royal Institute of Technology
SE-100 44 Stockholm, Sweden
skog@s3.kth.se

**ABSTRACT**

A GPS aided inertial navigation platform is presented, into which further sensors such as a camera, wheel-speed encoder etc., can be incorporated. The construction of the platform is described and an introduction to the sensor fusion approach is given. Results from a field-test is presented, indicating which error sources that needs to be modelled more accurately.

## 1. INTRODUCTION

The art of car racing is not only a question of having the most highly performable car, but also depends on the skills of the driver and the interaction between the driver and vehicle. This is a well known fact in professional car racing, such as Formula 1, where the behavior of both the car and the driver are constantly monitored for later analysis [1]. For other applications, such systems are far to costly and complex. However, a GPS aided inertial navigation system (INS) constructed around an off-the-shelf GPS receiver and a low-cost inertial measurement unit (IMU) could provide a lot of information about the behavior of the vehicle, for an acceptable cost. Apart from the direct information (position, velocity, acceleration and attitude) calculated by the GPS aided INS, more indirect information can be extracted as well. In [2], a vehicle movement visualizer together with a gear change detector based on the measured acceleration and attitude is described and implemented. In [3], the road bank angle and vehicle roll are estimated with a GPS aided INS.

An inertial navigation system is a dead reckoning navigation system, where the system's position, velocity and attitude are continuously calculated through integration of the accelerations and angular rates measured by the IMU. However, due to the integrative nature of the system, the INS has poor long-term accuracy. Small errors caused by biases and noise in the sensors accumulate with time and cause an unbounded position error. To the opposite of the INS is the GPS receiver an absolute navigation system and therefore has a bounded error. However, the GPS navigation solution is noisier than that of an INS, has a lower update rate ($\sim$ 1 Hz) and normally does not include attitude information [4]. By fusing data from a GPS and an INS, utilizing the two systems complimentary properties, a robust navigation system with both high accuracy and update rate may be obtained.




**Fig. 1**. *The front of the navigation platform with its touch screen. In the upper left corner there are four USB-, a RCA- and a RS232 serial-connector, for connection of external sensors, an external screen and a GPS receiver, respectively.*

During the last decade many papers about low-cost GPS aided systems for land vehicles have been written, see for example [5, 6] and the references therein. Most of the described work focus on the implemented algorithm used in the sensor fusion, and few give an overview of the total system and its construction and features. This paper gives an overview and presents preliminarily results from the construction of a portable low-cost GPS aided INS platform, intended to be used for example in car racing and driver training. The platform is constructed with the aim of creating a GPS aided INS application skeleton into which further sensors such as a camera, wheel-speed encoder etc., can easily be incorporated.

The outline of the paper is as follows: first, an overview of the platform is given in Section 2, describing its major building blocks and their features. Second, in Section 3 the sensors used in the navigation system are described. Focus is on the in-house constructed IMU hardware and its synchronization with the GPS-receiver. Next, in Section 4 the software algorithm used to fuse the sensor data is briefly described. In Section 5, preliminarily results from a first field test are presented, indicating which error-sources that



USAA-1029

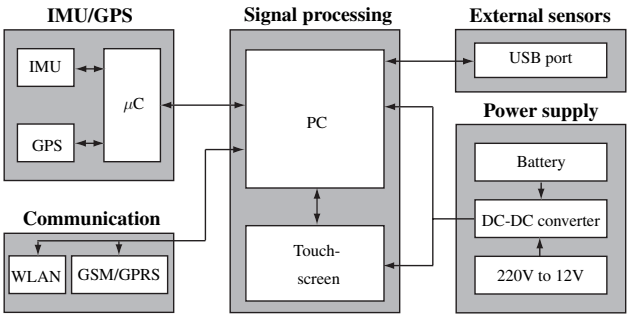



**Fig. 2**. *Block-diagram of the navigation platform. The platform is constructed around five modules.*

need to be more accurately modelled. Finally, in Section 6 conclusions and areas for further work are discussed.

## 2. SYSTEM OVERVIEW

The navigation platform in Figure 1 is designed with the aim of being both portable and robust, but still inexpensive. It is constructed around five blocks: signal processing, power supply, communication, IMU/GPS and the external sensors, see Figure 2.

The heart of the navigation platform is a Pentium-M 1.7 GHz PC, 512 MB RAM, 60 GB HD equipped with a 7" TFT touch screen. The PC handles all signal processing and interaction with the user. The PC and screen together with the IMU, power supply and wireless communication modules are built into an aluminium case, resulting in a robust system. The power supply module allows the platform to use three different power sources: the mains outlet (230 V AC), an external 11-15 V DC source, or internal batteries. The internal batteries allow for 2 hours stand alone operation of the navigation platform. The wireless communication module consists of a WLAN and GSM/GPRS connection, for real-time transmission of navigation data to remote applications as well as input from wireless sensors. Furthermore, an external GPS receiver is connected via a micro-controller to the PC. The micro-controller synchronizes the sampling of the GPS and IMU, as described in Section 3. The described hardware platform provides a skeleton for the development of a easy to use navigation platform.

## 3. SENSORS

The navigation platform is designed around the IMU and a GPS-receiver. However more sensors can be incorporated into the system through the USB-ports on the front of the navigation platform. Here, two auxiliary sensors are under special consideration, a vehicle speed encoder and a camera. The vehicle speed encoder gives the possibility to include a vehicle model in the sensor-fusion [7], improving the system performance in the absence of GPS-data. The camera provides visual information about the drivers reaction in different situations.

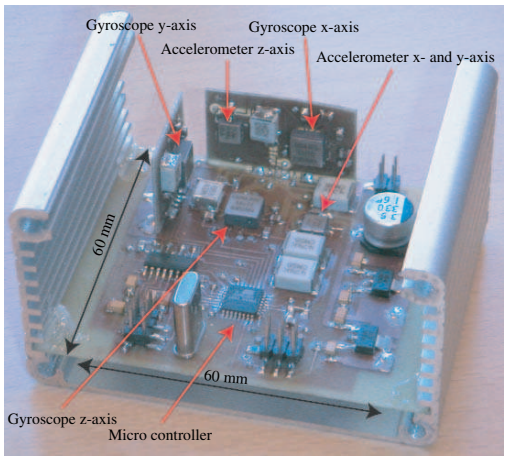



**Fig. 3**. *The inhouse constructed inertial measurement unit. In the upper part of the picture the three gyros and the double axed and single axed accelerometer can be seen. In the lower part of the picture the micro-controller can be seen, responsible for sampling of the sensors. Altogether the IMU measures 60×60×25 mm.*

With reference to Figure 3, the IMU has been constructed in-house around Micro-Electro-Mechanical System (MEMS) accelerometers and gyros from Analog-Devices. The double and single axled accelerometers ADXL 203 and ADXL 103, respectively have been mounted so that their sensitivity axes are nearly orthogonal and span a 3-dimensional space. Due to impreciseness in the construction, the sensitivity axes will not be perfectly orthogonal. The three ADXRS 150 gyros are mounted to measure the rotational velocity around the accelerometer's sensitivity axes. This gives a six degree-of-freedom IMU capable of measuring accelerations and angular rates between $\pm 1.5[g]$ and $\pm 150[^\circ/s]$, respectively. The sensors are controlled and sampled at a rate of 100 Hz by an AVR, ATmega 8 micro-controller, housing a built in 10-bit analog to digital converter. Further, the micro-controller also communicates with the GPS-receiver via a RS232 serial connection, synchronizing the sampling of the IMU and GPS. However, this synchronization does not take into account the processing delay inside the GPS-receiver, which may cause erroneous convergence of the integration algorithm [8]. The IMU and GPS data is enumerated by the controller and sent to the PC via a second RS232 serial connection.

Due to impreciseness in the mounting and construction of the MEMS sensors the IMU has some statical errors such as misalignment between the sensitivity axes, scale factors and biases [9]. These errors may be identified and compensated for, reducing the convergence time as well as the complexity of the integration algorithm. A description of a suitable IMU sensor model together with an evaluation of different algorithms for estimating the model parameters are given in [9, 10].

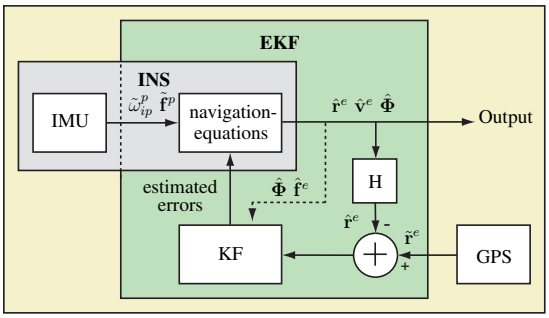



**Fig. 4**. *The INS provides the main navigation solution. When GPS data is available the position error is estimated and used as the input to a Kalman filter, estimating the navigation errors. The errors are fed back to the INS for correction of internal states.*

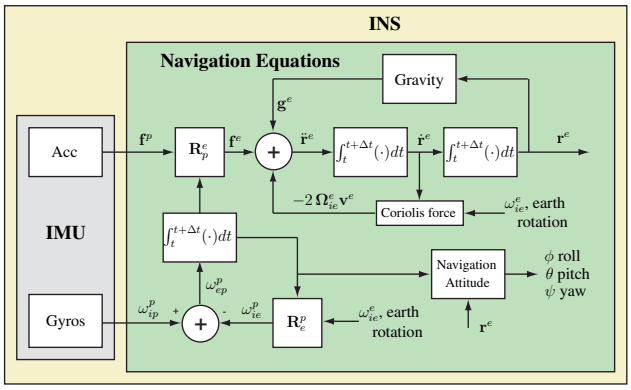



**Fig. 5**. *The block diagram corresponds to ECEF navigation equations used in the INS.*

## 4. SOFTWARE ALGORITHM

The algorithm for fusion of the INS and GPS data has previously been presented in [11], where a more thorough description can be found. In the used integration algorithm, the inertial navigation system provides the main navigation solution. Since the INS is an integrative process the output of the INS is the actual position and a predominantly low-frequency error. When a GPS position estimate is available the difference between the position estimate of the GPS and the INS is calculated. This error signal contains two noise components: the predominantly low-frequency INS component and the predominantly high-frequency GPS component [6]. The error signal is fed to a Kalman filter (KF), designed to attenuate the GPS measurement error and provide an estimate of the INS errors. Hence, the KF will mainly have a low-pass characteristic. The estimated INS error state is the feedback to the INS for correction of its internal states, see Figure 4. The INS and KF together forms an indirect extended Kalman filter (EKF), where the navigation equations are linearized around the current navigation output.

The continuous Earth-Centered-Earth-Fixed (ECEF) navigation equations used in the INS system to calculate position $\mathbf{r}^e$, velocity $\mathbf{v}^e$ and attitude $\mathbf{\Phi}$ from the accelerations $\mathbf{f}^p$ and angular rates $\omega_{ip}^p$ are

$$\dot{\mathbf{r}}^e = \mathbf{v}^e \tag{1}$$
$$\dot{\mathbf{v}}^e = \mathbf{R}_p^e\,\mathbf{f}^p - 2\,\mathbf{\Omega}_{ie}^e\,\mathbf{v}^e + \mathbf{g}^e \tag{2}$$
$$\dot{\mathbf{R}}_p^e = \mathbf{R}_p^e\,\mathbf{\Omega}_{ep}^p. \tag{3}$$

Here and in the sequel, the superscripts $e$, $p$, and $i$ denote in which coordinate-frame a quantity is expressed, the ECEF, platform and inertial frame, respectively. Further, $\mathbf{R}_p^e = \mathbf{R}_p^e(\mathbf{\Phi})$ denotes the directional cosine matrix transforming a vector from platform- to ECEF-coordinates. Note that the attitude $\mathbf{\Phi}$ can be calculated from $\mathbf{R}_p^e$ and *vice versa*. The matrices $\mathbf{\Omega}_{ep}^p$ and $\mathbf{\Omega}_{ie}^e$ are the skew symmetric matrix representations of $(\omega_{ep}^p\times)$ and $(\omega_{ie}^e\times)$, respectively. Here $(\times)$ denotes the cross-product operator. The rotational rate between the ECEF- and platform-coordinates, expressed in platform coordinates $\omega_{ep}^p$ may be calculated from the gyro measurements as $\omega_{ep}^p = \omega_{ip}^p - \mathbf{R}_p^e\omega_{ie}^e$. The earth rotational rate $\omega_{ie}^e$ is constant and may be calculated beforehand.

The interpretation of the navigation equations is illustrated in Figure 5. The angular rates measured by the gyros are used to keep track of the coordinate rotation matrix $\mathbf{R}_b^e$, i.e.s̃olving the difference equation in (3), transforming the specific-force measured in the platform-frame into a specific-force in the ECEF-frame. Next, the gravity $\mathbf{g}^e$ and coriolis force $2\mathbf{\Omega}_{ie}^e\mathbf{v}^e$ is subtracted. Remaining is then only the acceleration of the platform. Integrating the acceleration twice with respect to time, then the position in ECEF coordinates is obtained.

Through mechanization of the navigation equations and neglecting second and higher order terms a linear model relating the sensor errors $\delta\mathbf{f}^p$ and $\delta\omega_{ip}^p$ to the errors $\delta\mathbf{r}^e$, $\delta\mathbf{v}^e$ and $\delta\mathbf{\Phi}$ in the output of the INS may be found. Defining the errors as the perturbation between the calculated value and true value, respectively measured value and true value, then the error equations reads

$$\delta\mathbf{v}^e = \delta\dot{\mathbf{r}}^e \tag{4}$$
$$\delta\dot{\mathbf{v}}^e = -\mathbf{F}^e\,\delta\mathbf{\Psi} + \mathbf{R}_p^e\,\delta\mathbf{f}^p + \delta\mathbf{g}^e - 2\,\mathbf{\Omega}_{ie}^e\,\delta\mathbf{v}^e \tag{5}$$
$$\delta\dot{\mathbf{\Psi}} = \mathbf{R}_p^e\,\delta\omega_{ip}^p - \mathbf{\Omega}_{ie}^e\,\mathbf{\Psi}. \tag{6}$$

Here $\mathbf{F}^e$ is the skew symmetric matrix representation of $(\mathbf{f}^e\times)$ and $\delta\mathbf{g}^e$ is the error in the gravity vector. Worth noting is that the error equations depend on the current navigation state, i.e. $\mathbf{R}_p^e$ and $\mathbf{f}^e$. In [11] the navigation error equations are discretized and complimented with a model for how the sensor errors develop with time. A standard Kalman filter algorithm is applied to the error model, resulting in an indirect extended Kalman filter where the navigation equations are linearized around the output of the INS.

## 5. RESULTS

In Figure 6, the estimated trajectory (blue solid line) and GPS-receiver position estimates (red crosses) from a field




**Fig. 6**. *Estimated trajectory (blue solid line) and GPS-receiver position estimates (red crosses) from the field-test. The vehicle was kept stationary (see top) for the first 30 seconds and then drove along the highway southward.*

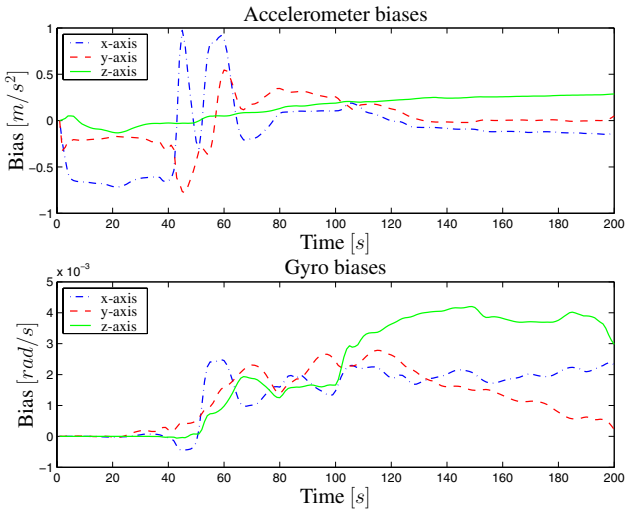



**Fig. 7**. *Estimated accelerometer and gyro biases during the field test. The accelerometer biases start converging directly, while the gyro biases are unobservable when the vehicle is stationary during the first 30 seconds.*

test of the navigation platform is shown. The vehicle was kept stationary for 30 seconds, then made a wide turn and headed along a highway for approximately 3 minutes. No GPS outages occurred during that time, although the position dilution of precision (PDOP) reached values as high as 40 at a few points. 72% of the time the PDOP value was below 5, which can be considered as acceptable.

The IMU sensor errors were modelled as constants in the integration algorithm, i.e.ã bias in the measured accelerations and rotational rates. In Figure 7, the estimated sensor biases from the field test are shown. After approximately 120 seconds, the accelerometer biases have converged. However, there are convergence problems for the gyro biases and a linear growth in the heading error. Possible error sources can be identified in the misalignment of the gyros and a delay between the GPS estimates and IMU samples [8], respectively. An exact position error evaluation is not possible due to the lack of reference trajectory data.

## 6. CONCLUSIONS AN FURTHER WORK

A versatile GPS aided inertial navigation platform, into which more sensors easily can be incorporated has been described. The use of a standard PC as a signal processing engine gives a navigation platform with extensive processing power for a low-cost, as well as the possibilities to run other applications. Further, the use of a PC allows the navigation software developers to develop the software modules for new sensors on their own computer, and then port it to the navigation platform without the need to consider the hardware specific properties

Concerning the navigation algorithm, the error model needs to be extended to take into account more error sources such as the sensor's scale factors and the delay in the GPS receiver. In addition, through pre-calibration of the IMU the misalignment between the accelerometer and gyro sensitivity axes should be estimated and compensated.

Further work will focus on incorporating a vehicle model together with a velocity encoder into the sensor fusing algorithm. Methods for online estimation of the GPS processing delay will be studied.

## 7. REFERENCES


[1] L. Boland "Formula 1 racing: The Xilinx advantage," in *Xcell Journal.*, pp. 46 – 49, Fall 2003.

[2] H. Grunell "Visualization and analysis of vehicle movement and driving performance using inertial navigation," Technical Report, *Dept. of Signals, Sensors and Systems*, Royal Institut of Technology, Sweden, 2005.

[3] J. Ryu and J. C. Gerdes "Estimation of vehicle roll and road bank angle," in *Proc. Amer. Cont. Conf.*,MA, 2004, pp. 2110–2115.

[4] B. Boberg "Robust navigation," in *Swedish Journal of Military Technolgy*, pp. 46 – 49, Fall 2003.

[5] R. Dorobantu and B. Zebhauser, "Field evaluation of a low-cost strapdown IMU by means GPS," in *Ortung und Navigation, DGON, Bonn*, 1999, nr. 1, pp. 51 – 65.

[6] J. A. Farrell, T. D. Givargis and M. J. Barth "Real-time differential carrier phase GPS-aided INS," *IEEE. Trans. Cont. Syst. Thechnol.*, vol. 8, pp. 709 – 721, 2000.

[7] G. Dissanayake, S Sukkarieh, E. Nebot and H. D. Whyte "The aiding of a low-cost strapdown inertial measurement unit using vehicle model constraints for land vehicle applications," *IEEE. Trans. Robotics and Automation*, vol. 17, pp. 731 – 747, 2001.

[8] H. K. Lee, J. G. Lee and G. Jee "Calibration of measurement delay in global positioning system/strapdown inertial navigation system," in *Jour. of Guid. Cont. and Dyn.*, vol. 25, nr. 2, pp. 240–247, 2002.

[9] A. Kim and M.F Golnaraghi "Initial calibration of an inertial measurement unit using an optical position tracking system", in *Proc. PLANS 2004, IEEE Position Location and Navigation Symposium*, 26–29 April. 2004, pp. 96 – 101.

[10] I. Skog and P. Händel, "Calibration of a MEMS inertial measurement unit, IMEKO XVIII World Congress, September 17-22, 2006, Rio de Janerio, Brazil.

[11] I. Skog, P. Händel " A low cost GPS aided INS for vehicles," in, *Proc. EUSIPCO 2005*, September 4–8, 2005, Antalya, Turkey.